

# Numerical Modelling of Porous Square Cavity Heated on Vertical Walls in Presence of Magnetic Field



L. Jino, A. Vanav Kumar, Swapnali Doley, M. Berlin, and P. K. Mohanty

## 1 Introduction

An investigation of natural convection in a fluid flow via a porous media was increasing because of many engineering applications such as separation process in a chemical industries, crystal growth structure, phase change applications, dispersion of chemical contaminant in a through water and geophysics [1–3]. The natural convective flow through the porous media with the effect of magnetic field is governed by non-dimensional parameters such as Rayleigh number  $Ra$ , Darcy number  $Da$ , Prandtl number  $Pr$ , and Hartmann number  $Ha$ . Note that,  $Ra$  denotes the natural convective effect, porosity by  $Da$  and magnetic field strength by  $Ha$ , respectively. A comprehensive study is found in the references [4, 5].

Basak et al. [6, 7] discussed the effect of natural convection in a porous cavity for the various thermal boundaries such as constantly heated, linearly heated and sinusoidally heated. An increase in  $Ra$  leads to conversion of conduction dominant flow to the convection dominant flow, and also increase in  $Da$  motivates the circulation intensities. Natural convection heat transfer in a nanoparticle into a fluid saturated porous media is presented by Groşan et al. [8]. Sheikholeslami [9, 10] investigated the influence of magnetic field in a different shaped porous cavities filled with nanofluid. The results denote that increase in the nanofluid solid volume fraction  $\phi$ ,  $Ra$ ,  $Da$  enhances the heat transfer and increase in the  $Ha$  reduces the heat transfer. Also, the

---

L. Jino · A. Vanav Kumar (✉) · S. Doley

Department of Basic and Applied Science, National Institute of Technology Arunachal Pradesh, Yupia, India

M. Berlin

Department of Civil Engineering, National Institute of Technology Arunachal Pradesh, Yupia, India

P. K. Mohanty

Department of Mechanical Engineering, National Institute of Technology Arunachal Pradesh, Yupia, India

increase in the Darcy number from  $10^{-2}$  to  $10^2$  changes the shape of the streamlines and increases the flow rushing. Rashad et al. [11] investigated the effect of heat generation and magnetic field in a porous cavity saturated with Cu-water nanofluid. The results shows that, increase in the  $Ha$  and  $\phi$  reduces the average Nusselt number and increase in Hartmann number increases the maximum temperature while it reduces the flow circulation intensity. Kumar et al. [12, 13] investigated the fluid flow due to natural convection in a porous square cavity with sinusoidally and partially heated boundaries. Jino and Vanav [14] discussed the heat flow, fluid flow and nanoparticle concentration generated due to the magneto-hydrodynamics natural convection in a porous cavity using Carman–Kozeny equation model.

Teamah and El-Maghlany [15] discussed natural convective on magnetic field and heat generation, absorption in a square cavity. Ghasemi et al. [16] in their study concluded that an increase in  $\phi$  causes increase of drop in heat transfer performance depending upon the value of  $Ha$  and  $Ra$  selected. Rudraiah et al. [17] studied the magnetic field effects on natural convective cavity. The rate of convection is reduced by increasing the Hartmann number and reduces the average Nusselt number in an electrically conducting fluid.

In this study, the effect magnetic field on natural convective porous cavity filled with the Cu-water nanofluid is carried out. The Carman–Kozeny equation model is used to model the fluids passes via porous media.

## 2 Problem Description

A cavity ( $H \times H$ ) is filled with the Cu-water nanofluid ( $Pr = 6.2$ ) in a two-dimensional cartesian coordinate system with higher wall temperatures in both the vertical walls and lower temperature at the bottom wall. The top side wall temperature of the cavity is maintained adiabatically as shown in Fig. 1.

The nanofluid is assumed to be Newtonian, incompressible and laminar with the validation of Boussinesq approximation. Here, the water is considered as the base fluid containing the Cu nanoparticle. The thermo-physical properties of Cu-water nanofluid is listed in Table 1. The gravity acts parallel to the vertical walls, and the induced magnetic field is negligible when compared to the applied magnetic field.

## 3 Mathematical Model

The governing equations are made to fluid and heat flow in a cavity by the conservation of mass, momentum and energy with the applicable assumptions made above as,

$$\frac{\partial u}{\partial x} + \frac{\partial v}{\partial y} = 0 \quad (1)$$

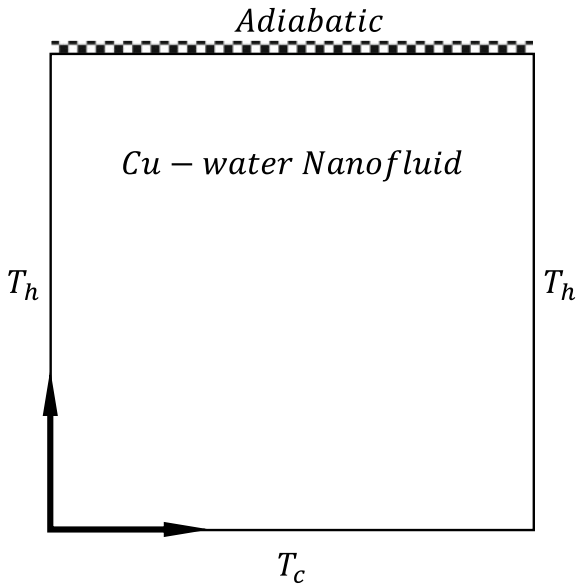


Fig. 1 Physical model

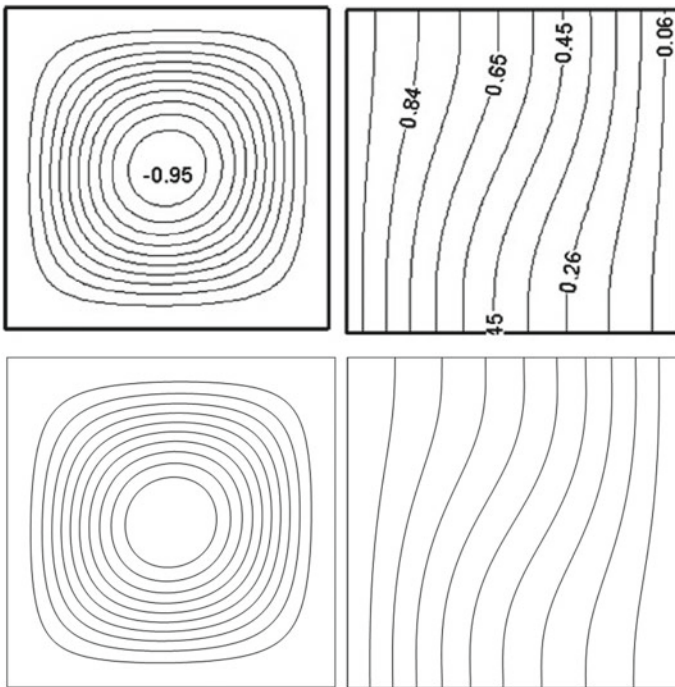


Fig. 2 Code validation of streamlines (left) and isotherm (right) contours of present study (bottom) to that of Ghasemi et al. [16] (top)

**Table 1** Properties of water and Cu nanoparticle

	Water	Cu particle
$\rho$ (kg/m <sup>3</sup> )	997.1	8954
$\mu$ (Pa s)	$8.9 \times 10^{-4}$	–
$c_p$ (J/kg K)	4179	383
$k$ (W/m K)	0.6	400
$\beta$ (K <sup>-1</sup> )	$2.1 \times 10^{-4}$	$1.67 \times 10^{-5}$

$$\rho_n \left[ u \frac{\partial u}{\partial x} + v \frac{\partial u}{\partial y} \right] = \mu_n (\nabla^2 \cdot \mathbf{u}) - F_x \quad (2)$$

$$\rho_n \left[ u \frac{\partial v}{\partial x} + v \frac{\partial v}{\partial y} \right] = \mu_n (\nabla^2 \cdot \mathbf{v}) - F_y \quad (3)$$

$$(\rho c_p)_n \left[ u \frac{\partial T}{\partial x} + v \frac{\partial T}{\partial y} \right] = k_n (\nabla^2 \cdot \mathbf{T}) \quad (4)$$

Here  $F_y = -\partial p/\partial y - \rho_n [C_m(1-\lambda)]^2/\lambda^3 v - \sigma_n B^2 v + (\rho\beta)_n g(T - T_0)$  and  $F_x = -\partial p/\partial x - \rho_n [C_m(1-\lambda)]^2/\lambda^3 u$ .  $u$ ,  $v$  are velocities,  $p$  is pressure and  $T$  is temperature with the directions  $x$  and  $y$ . The fluid in a porous media is controlled by the porosity constant ( $C_m$ ) and liquid fraction ( $\lambda$ ).  $B$  is the applied magnetic field. The other parameters such as electrical conductivity, density, viscosity, thermal conductivity, specific heat and thermal expansion coefficient depend on the amount of solid volume fraction of the Cu nanoparticle [13].

The above two-dimensional dimensional governing equations Eqs. (1–4) are modified into the non-dimensional governing equation as,

$$\frac{\partial U}{\partial X} + \frac{\partial V}{\partial Y} = 0 \quad (5)$$

$$U \frac{\partial U}{\partial X} + V \frac{\partial U}{\partial Y} = \frac{\mu_n}{\rho_n \alpha_{fl}} \left( \frac{\partial^2 U}{\partial X^2} + \frac{\partial^2 U}{\partial Y^2} \right) - F_x \quad (6)$$

$$U \frac{\partial V}{\partial X} + V \frac{\partial V}{\partial Y} = \frac{\mu_n}{\rho_n \alpha_{fl}} \left( \frac{\partial^2 V}{\partial X^2} + \frac{\partial^2 V}{\partial Y^2} \right) - F_y \quad (7)$$

$$U \frac{\partial \theta}{\partial X} + V \frac{\partial \theta}{\partial Y} = \frac{\alpha_n}{\alpha_{fl}} \left( \frac{\partial^2 \theta}{\partial X^2} + \frac{\partial^2 \theta}{\partial Y^2} \right) \quad (8)$$

Non-dimensional source terms  $F_y = -\partial P/\partial Y - \rho_{fl}(\text{Pr}/\text{Da})V + (\rho\beta)_n/(\rho_n \beta_{fl})\text{RaPr}\theta - \text{Ha}^2\text{Pr}V$  and  $F_x = -\partial P/\partial X - \rho_{fl}(\text{Pr}/\text{Da})U$ , respectively. The non-dimensional variables are  $X = x/H$ ,  $Y = y/H$ ,  $U = (uH)/\alpha_f$ ,  $V = (vH)/\alpha_f$ ,  $P = (pH^2)/(\rho_n \alpha_f^2)$  and  $\theta = (T - T_0)/(T_h - T_0)$ . The other non-dimensional numbers such as Prandtl number ( $\text{Pr} = \nu_f/\alpha_f$ ), Darcy

number  $Da = (\mu_f \lambda^3)/(C_m (1 - \lambda)^2 H^2)$  to control the porosity, Rayleigh number  $Ra = (g\beta_f H^3 (T_h - T_c))/(\nu_f \alpha_f)$  responsible for natural convection effects, and intensity of magnetic field by Hartmann number  $Ha = Bl\sqrt{\sigma_n/(\rho_n \nu_n)}$ .

The flow governing equations are solved by the essential boundary conditions such as  $(\theta = 1)$  for higher temperature walls,  $(\theta = 0)$  for lower temperature wall and adiabatic wall as  $(\partial\theta/\partial n = 0)$ . The no-slip velocity  $(U = V = 0)$  boundaries are imposed on all the walls.

The fluid motion in the cavity is visualized using the streamlines which are obtained from the velocities  $U = (\partial\psi/\partial Y)$  and  $V = -(\partial\psi/\partial X)$ .

The heat transfer enhancement of the convective to the conductive heat transfer at the wall is denoted by the dimensionless quantity local Nusselt number,  $Nu = -(k_n/k_{fl})(\partial\theta/\partial n)$ .

## 4 Numerical Description

The streamlines  $\psi$  from the velocities  $U, V$  and isotherms  $\theta$  are solved using the second order of finite different method in a  $100 \times 100$  constant spaced computational domain. The governing equations Eq. (5–8) are formulated into vorticity–stream-function, which are solved using the respective boundary conditions. The solutions are formed using the iterative process and iteration can be done till the convergence criteria  $(|(\xi^{n+1} - \xi^n)/\xi^{n+1}| < 10^{-5})$  for temperature and velocities. Here,  $n$  represents the iteration number.

The validation of code has been performed for effect of magnetic field on natural convection in a square cavity filled with nanofluid. The results obtained are quite similar to the work of Ghasemi et al. [16]. The grid independence study is carried out (ref Fig. 3), and constant grid of  $100 \times 100$  is considered in this entire study.

## 5 Results and Discussion

The numerical result presents the streamlines and isotherms of Cu-water nanofluid for the various values of  $10^3 \leq Ra \leq 10^5$  with the constant volume fraction of the particle  $\phi = 0.1$ , within the Darcy number  $10^{-2} \leq Da \leq 10^2$ . The applied magnetic field strength in a cavity is indicated by Hartmann number  $0 \leq Ha \leq 50$ . The local Nusselt number (Nu) is calculated at heated vertical walls for Ra with respect to the Darcy number and Hartmann number.

Figure 4 represents the flow structure of streamlines and isotherms at  $Ra = 10^4$  for various Da and Ha. The flow in a cavity initiates by the temperature difference and has the symmetry flow pattern in both the side vertical orientation with anti-clockwise and clockwise rotation. The variation of rotation is due to the difference in temperature distribution of higher to lower temperature and lower to higher temperature of bottom and vertical walls. At the lower Darcy number, the flow rush is low and increased

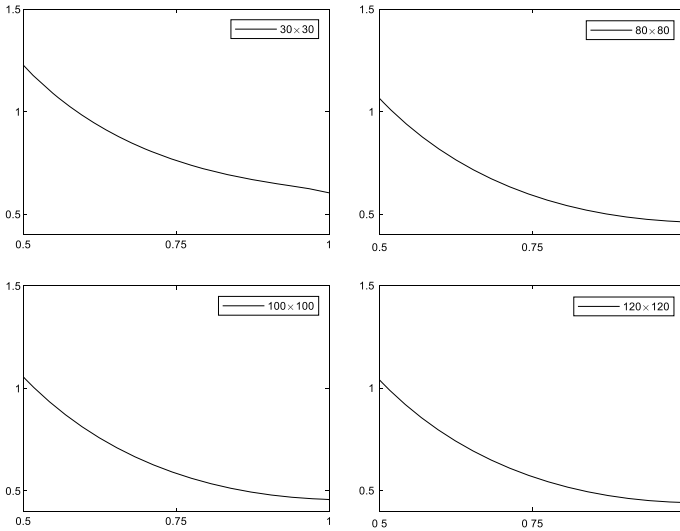


**Fig. 3** Grid independency study

for increase in the  $Da$  from  $10^{-2}$  to  $10^2$ . The isotherm also flows from both the vertical walls symmetrically towards the mid-plane without any collaboration. The higher Darcy number makes increase in flow rush, and the isotherm that moves from the vertical walls is merged and makes the temperature distribution from the lower bottom to top cavity linearly.

The effect of Hartmann number has a very less sense at the lower  $Da$  in both the streamlines and the isotherms but at the  $Da = 10^2$  the increase in the  $Ha$  suppresses the flow rush. The isotherm at top separated because of reduction in the heat transfer rate at the  $Ha = 50$ .

The  $Ra = 10^5$  is set, so that the natural convective effect is increased and the flow rush also increases than before and isotherm also merged half and distributed. An increase in the Hartmann number has very minor change in the streamlines and in isotherm, the temperature distribution ( $\theta = 0.5$ ) small elongation towards the adiabatic wall at  $Da = 10^{-2}$  as shown in Fig. 5. When increasing the Darcy number, the flow rush is increased more as discussed previously, and the temperature distribution from the vertical wall is more. The increase in the  $Ha = 50$  leads to reduce in flow rush and push towards the bottom. The temperature deviation also reduces as compared to  $Ha = 0$ .

The local Nusselt number for the left isothermal wall is shown in Fig. 6.  $Nu$  is more for  $Da = 10^{-2}$  at lower Rayleigh number and decreases for increasing in the  $Ra$ . But  $Nu$  is less for same Rayleigh number as Darcy number increased to  $10^2$  because at  $Da = 10^{-2}$  the conduction effects are more dominant. The increase in the  $Ra$  gradually decreases in  $Nu$  for smaller  $Da$  and increases for higher  $Da$ . At when Rayleigh number reaches to  $10^5$ , the Nusselt number becomes almost similar for both the  $Da = 10^{-2}$  and  $10^2$ . The effect of applied magnetic field leads to the slight

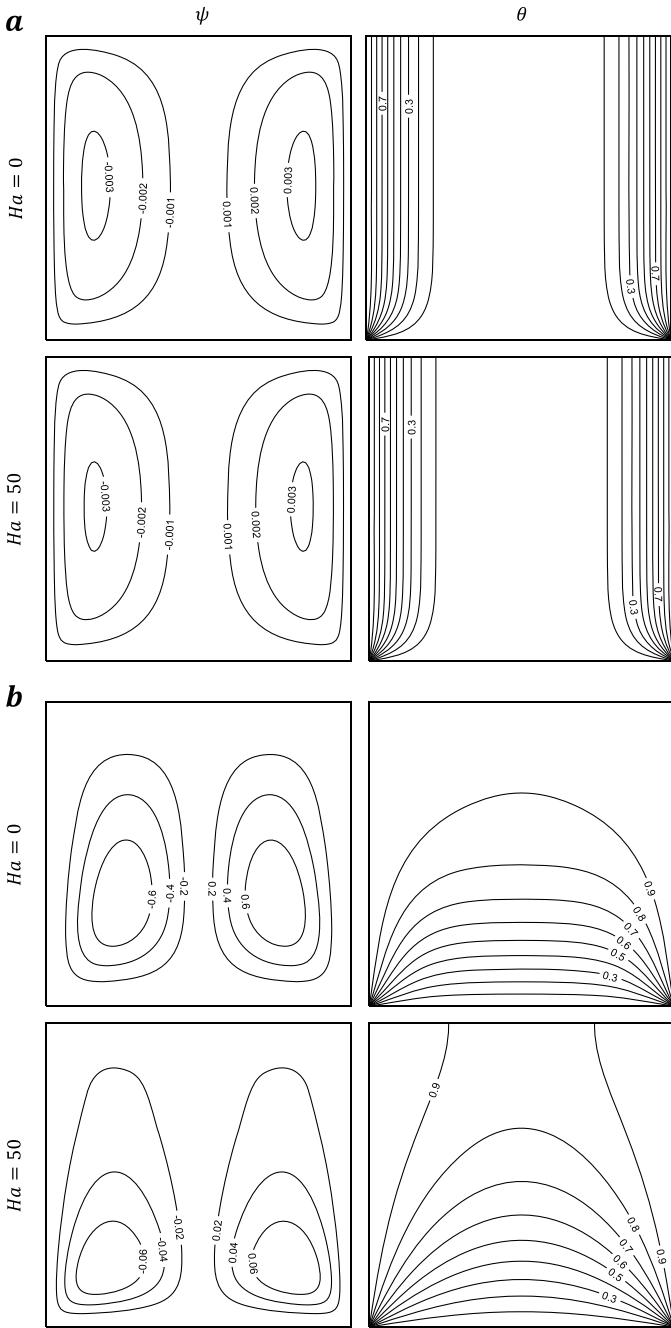
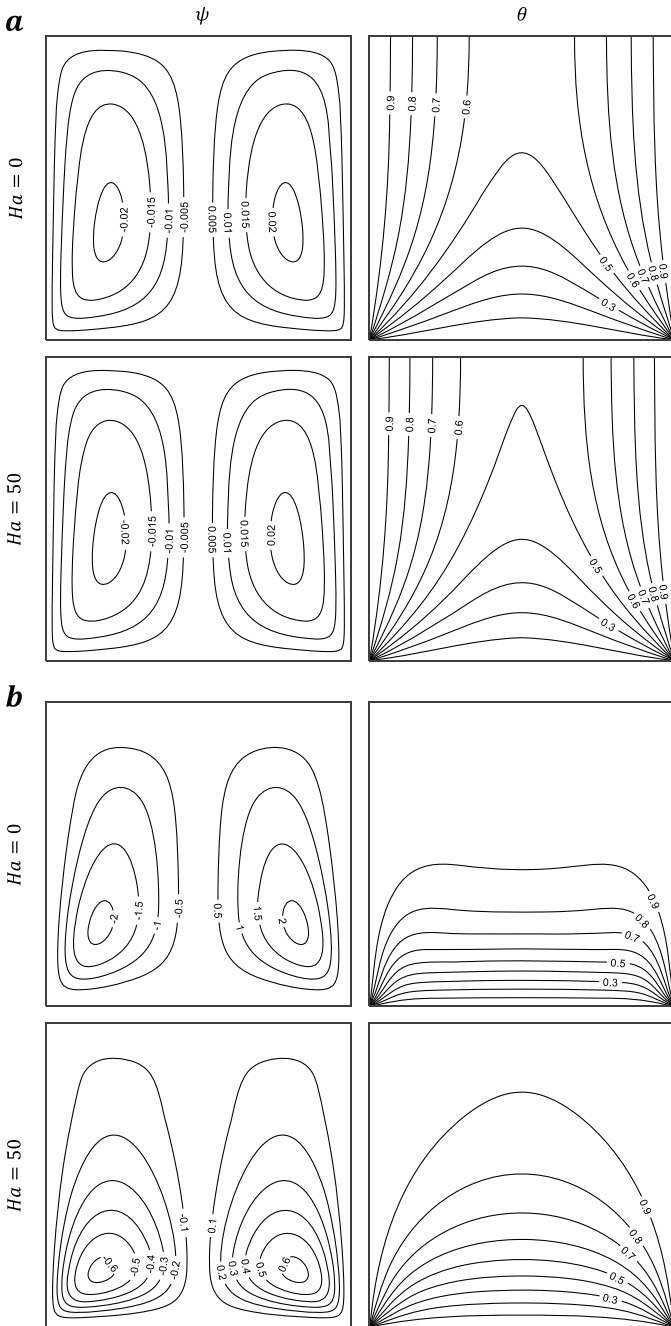
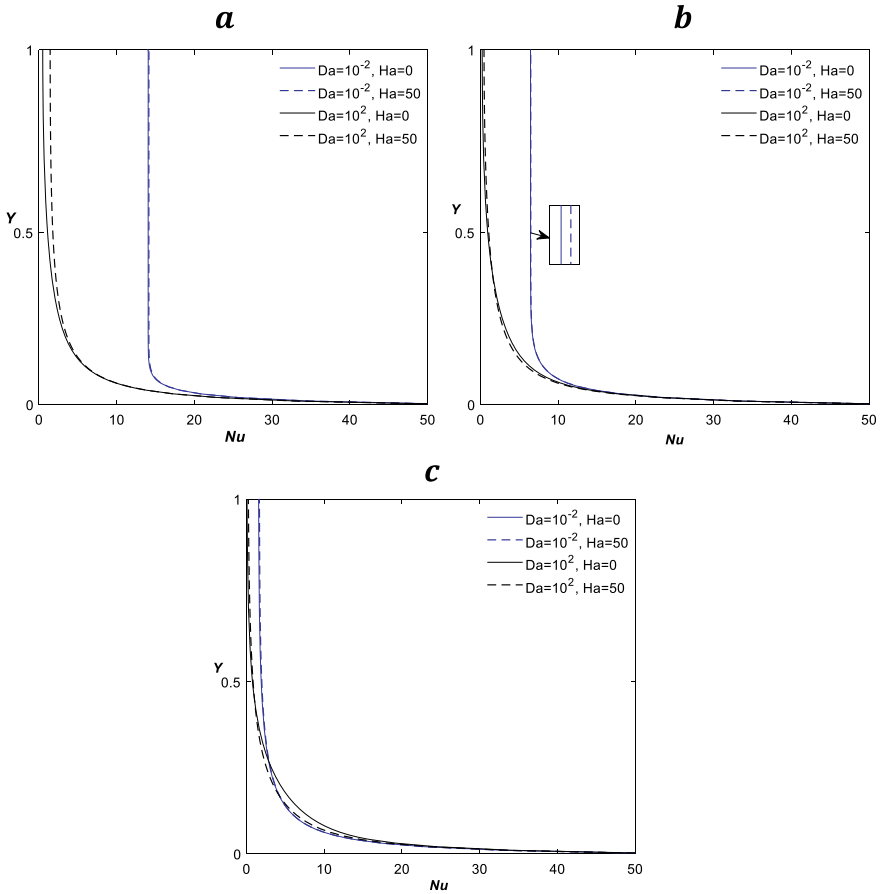


Fig. 4 Streamfunction and temperature contours for  $Ra = 10^4$  with **a**  $Da = 10^{-2}$  and **b**  $Da = 10^2$



**Fig. 5** Streamfunction and temperature contours for  $Ra = 10^5$  with **a**  $Da = 10^{-2}$  and **b**  $Da = 10^2$





**Fig. 6** Local Nusselt number for **a**  $Ra = 10^3$ , **b**  $Ra = 10^4$  and **c**  $Ra = 10^5$  at left wall

increase in  $Nu$  for lower Darcy number and for  $Da = 10^{-2}$ , initially at  $Ra = 10^3$  the  $Nu$  increases and decreases for further increase in the  $Ra$  because of domination of natural convection effects. The  $Nu$  at the bottom increases at the vertical walls because of discontinuity in temperature from higher temperature to lower temperature. The variation in a local Nusselt number is same for both the vertical walls.

## 6 Conclusion

The flow modelling of Cu-water nanofluid in a porous cavity is studied numerically using the various Darcy number due to natural convection. The magnetic field strength is introduced by varying the Hartmann number from 0 to 50. The increase in the Darcy

number leads to the decrease in the heat transfer rate at lower Ra and vice versa at for higher Rayleigh number. The effect of  $Ha = 50$  leads to a minor increase in Nu for lower Darcy number and decreases slightly for  $Da = 10^2$  except when  $Ra = 10^3$ . The flow rush in a cavity is more for higher Darcy number and magnetic field effect reduces it rush. At lower Darcy number, only negligible flow field change occurs for increase in the Ha.

**Acknowledgements** The authors acknowledge the financial support through TEQIP-III for presenting this work.

## References

1. Bejan, A. (2006). *Convection in porous media*. Springer.
2. Ingham, D. B., & Pop, I. (1998). *Transport phenomena in porous media*. Elsevier.
3. El Hasadi, Y. M. F., & Khodadadi, J. M. (2013). *Journal of Heat Transfer*. <https://doi.org/10.1115/1.4023542>
4. Bejan, A., Dincer, I., Lorente, S., Miguel, A., & Reis, H. (2004). *Porous and complex flow structures in modern technologies*. Springer.
5. Kasaeian, A., Azarian, R. D., Mahian, O., Kolsi, L., Chamkha, A. J., Wongwises, S., & Pop, I. (2017). Nanofluid flow and heat transfer in porous media: A review of the latest developments. *International Journal of Heat and Mass Transfer*, 107, 778–791. <https://doi.org/10.1016/j.ijheatmasstransfer.2016.11.074>
6. Sathiyamoorthy, M., Basak, T., Roy, S., & Pop, I. (2007). Steady natural convection flow in a square cavity filled with a porous medium for linearly heated side wall(s). *International Journal of Heat and Mass Transfer*, 50, 1892–1901. <https://doi.org/10.1016/j.ijheatmasstransfer.2006.10.010>
7. Basak, T., Roy, S., Paul, T., & Pop, I. (2006). Natural convection in a square cavity filled with a porous medium: Effects of various thermal boundary conditions. *International Journal of Heat and Mass Transfer*, 49, 1430–1441. <https://doi.org/10.1016/j.ijheatmasstransfer.2005.09.018>
8. Groşan, T., Revnic, C., Pop, I., & Ingham, D. B. (2015). Free convection heat transfer in a square cavity filled with a porous medium saturated by a nanofluid. *International Journal of Heat and Mass Transfer*, 87, 36–41. <https://doi.org/10.1016/j.ijheatmasstransfer.2015.03.078>
9. Sheikholeslami, M. (2017). Influence of magnetic field on nanofluid free convection in an open porous cavity by means of Lattice Boltzmann method. *Journal of Molecular Liquids*, 234, 364–374. <https://doi.org/10.1016/j.molliq.2017.03.104>
10. Sheikholeslami, M. (2017). Numerical simulation of magnetic nanofluid natural convection in porous media. *Physics Letters, Section A: General, Atomic and Solid State Physics*, 381, 494–503. <https://doi.org/10.1016/j.physleta.2016.11.042>
11. Rashad, A. M., Rashidi, M. M., Lorenzini, G., Ahmed, S. E., & Aly, A. M. (2017). Magnetic field and internal heat generation effects on the free convection in a rectangular cavity filled with a porous medium saturated with Cu–water nanofluid. *International Journal of Heat and Mass Transfer*, 104, 878–889. <https://doi.org/10.1016/j.ijheatmasstransfer.2016.08.025>
12. Kumar, A. V., Jino, L., Berlin, M., & Mohanty, P. K. (2019). Magnetic field effect on nanofluid suspension cavity by non-uniform boundary conditions. *AIP Conference Proceedings AIP Publishing*. <https://doi.org/10.1063/1.5120205>
13. Jino, L., & Vanav Kumar, A. (2020). Natural Convection of Water-Cu Nanofluid in a Porous Cavity with Two Pairs of Heat Source-Sink and Magnetic Effect. *International Journal of Mechanical and Production Engineering Development*, 10, 14481–14492. <https://doi.org/10.24247/ijmperdjun20201378>

14. Jino, L., & Vanav Kumar, A. (2020). Cu-water nanofluid natural convective heat and fluid flow in a porous cavity. *International Journal of Mechanical and Production Engineering Research Development*, 10, 13695–13706. <https://doi.org/10.24247/ijmperdjun20201305>
15. Teamah, M. A., El-Maghlany, W. M. (2012). Augmentation of natural convective heat transfer in square cavity by utilizing nanofluids in the presence of magnetic field and uniform heat generation/absorption. *International Journal of Thermal Sciences*, 58, 130–142. <https://doi.org/10.1016/j.ijthermalsci.2012.02.029>
16. Ghasemi, B., Aminossadati, S. M., & Raisi, A. (2011). Magnetic field effect on natural convection in a nanofluid-filled square enclosure. *International Journal of Thermal Sciences*, 50, 1748–1756. <https://doi.org/10.1016/j.ijthermalsci.2011.04.010>
17. Rudraiah, N., Barron, R. M., Venkatachalappa, M., & Subbaraya, C. K. (1995). Effect of a magnetic field on free convection in a rectangular enclosure. *International Journal of Engineering Science*, 33, 1075–1084. [https://doi.org/10.1016/0020-7225\(94\)00120-9](https://doi.org/10.1016/0020-7225(94)00120-9)